Separation Science and Technology
Publication details, including instructions for authors and subscription information:
http://www.informaworld.com/smpp/title~content=t713708471

Modeling in-situ Protein Separation by Bubble Fractionation in a Baker's Yeast Fermentation Process

F. John Potter[a]; Arun H. G. Desouza[a]; Robert D. Tanner[a]; David J. Wilson[b]
[a] DEPARTMENT OF CHEMICAL ENGINEERING, [b] DEPARTMENT OF CHEMISTRY, VANDERBILT UNIVERSITY, NASHVILLE, TENNESSEE

To cite this Article Potter, F. John , Desouza, Arun H. G. , Tanner, Robert D. and Wilson, David J.(1990) 'Modeling in-situ Protein Separation by Bubble Fractionation in a Baker's Yeast Fermentation Process', Separation Science and Technology, 25: 6, 673 — 687
To link to this Article: DOI: 10.1080/01496399008050358
URL: http://dx.doi.org/10.1080/01496399008050358

SEPARATION SCIENCE AND TECHNOLOGY, 25(6), pp. 673-687, 1990

Modeling *in-situ* Protein Separation by Bubble Fractionation in a Baker's Yeast Fermentation Process*

F. JOHN POTTER, ARUN H. G. DeSOUZA, and ROBERT D. TANNER†

DEPARTMENT OF CHEMICAL ENGINEERING

DAVID J. WILSON

DEPARTMENT OF CHEMISTRY

VANDERBILT UNIVERSITY
NASHVILLE, TENNESSEE 37235

Abstract

Proteins produced by yeast have been observed to stratify in the extracellular fluid of a batch bioreactor, creating a vertical concentration gradient. The gradient in the bioreactor exists even when other parameters (such as the cell concentration and pH) indicate that the system is well mixed. The stratification appears to be the result of bubble fractionation, with proteins adsorbing onto and being transported by gas bubbles to the liquid surface. In addition, it seems that bubbles entrain a liquid layer of significant thickness which contains soluble protein. Sparging the system with gas accentuates the separation, but even in a nonsparged system the *in-situ* generation of minute carbon dioxide bubbles by yeast cells creates a protein concentration gradient as the bubbles carry proteins upward.

INTRODUCTION

The observation of protein stratification in the broth during a fermentation process has been previously observed (*1, 2*). This stratifiction was first

*Presented at the 8th International Biotechnology Symposium, Paris, France, July 19, 1988.

†To whom correspondence should be addressed.

noted because measurements of protein concentrations in a tall 1-L beaker under identical conditions were difficult to duplicate unless the samples were taken at the same depth in the beaker (*1*). The data analyzed in this paper are taken from a subsequent report of extracellular total protein stratification in a tall 1-L graduated cylinder (*3*).

The apparatus to be analyzed is a vertical cylinder containing an aqueous solution of proteins in a fermentation growth medium at T = 32°C and 1 atm pressure. The solution may also contain yeast cells and excess NaCl. The extracellular protein concentration varies from 40 to 300 g/L total protein, although for a given fermentation process the absolute variation of the concentration of total protein in the extracellular fluid did not vary more than 60% from the average concentration. This concentration is low enough that a stable foam does not form at the top of the column; therefore, any protein carried upward by a bubble is released at the liquid surface and allowed to disperse downward. This relatively constant total extracellular protein concentration means that each fermentation run may be modeled, to a first approximation, as if the cell level remains constant and as if there is not protein degradation (proteolysis) or generation (synthesis).

METHODOLOGY

Figure 1 illustrates the physical system. Sample ports at the bottom, middle, and top of the cylinder allow removal of samples for analysis without significantly disturbing the bubble flow patterns (*3*). Total proteins were quantified by the Bradford Coomassie Blue method (*3*). The pH and total cell mass were also measured (*3*).

STEADY-STATE MATHEMATICAL MODEL

This model was developed to describe measured extracellular total protein concentrations (from Ref. *3*) in a 1-L graduated cylinder, with sampling points at the bottom ($z = 0$), middle ($z = H/2$), and top ($z = H$). The following assumptions are made in developing the model:

(a) The bulk liquid is stagnant (the liquid velocity in any direction is low relative to the bubble rise velocity).

(b) The bubble rise velocity is constant and can be predicted by Stokes' law.

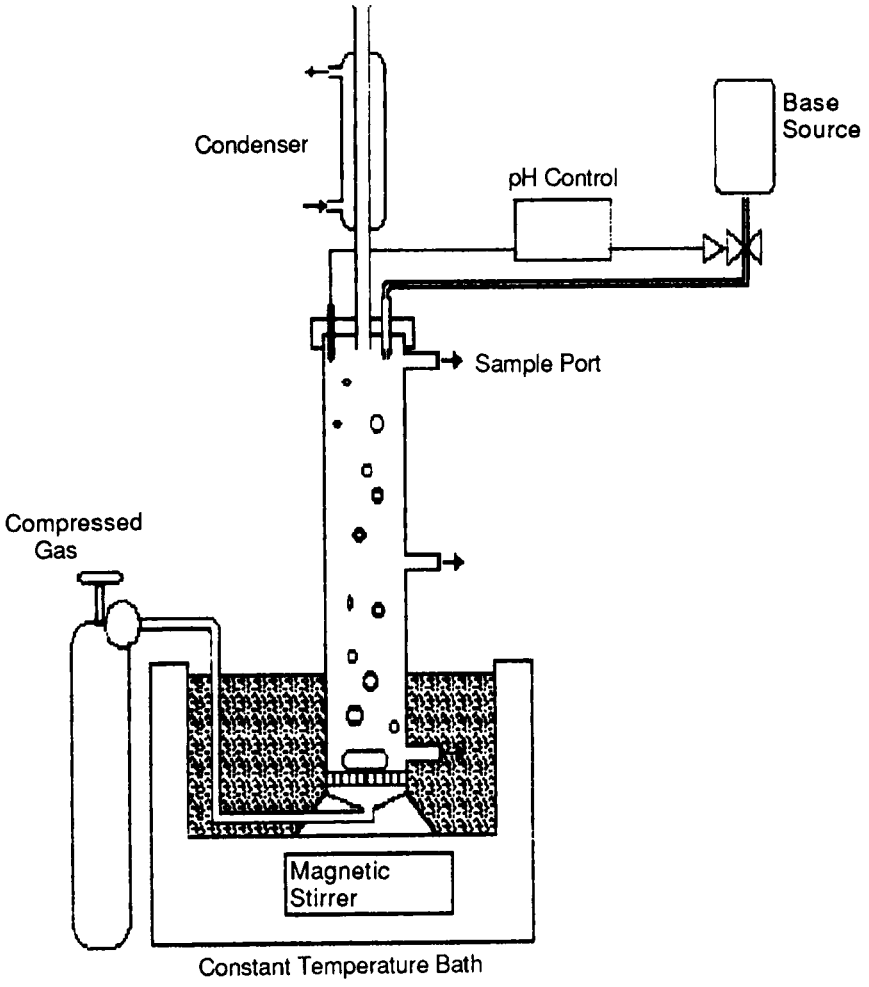

FIG. 1. Bubble fractionation/fermentation apparatus diagram (from Ref. 3).

(c) Quasi-steady-state behavior is reached at a rate which is rapid compared to the rate of extracellular protein production.

(d) The proteins have already been synthesized by the yeast and only need to be separated (i.e., the extracellular protein level can be considered to be independent of time, as a first approximation).

The bubble surface concentration of protein is related to the bulk liquid protein concentration by assuming local equilibrium and using a Langmuir isotherm in the low protein concentration range. This gives an equation analogous to Henry's law:

$$\Gamma = KC \tag{1}$$

where Γ = bubble surface protein concentration, mg/cm^2
C = bulk liquid protein concentration, mg/cm^3
K = equilibrium adsorption isotherm constant, cm

At steady-state conditions the protein flux upward equals the protein flux downward. The protein flux upward, F_{up}, is the amount of protein carried per bubble times the number of bubbles released per second, divided by the cross – sectional area of the column:

$$F_{up} = \frac{3QKC}{r\pi R^2}$$

The protein flux downward is due to dispersion alone, and it can be represented by the product of the effective dispersion coefficient times the protein concentration gradient in the bulk liquid. This is

$$F_{down} = DdC/dz$$

Equating these fluxes then yields

$$\frac{dC}{dz} - \frac{3QKC}{Dr\pi R^2} = 0 \tag{2}$$

where D = protein dispersion coefficient, cm^2/s
r = bubble radius, cm
Q = gas flow rate, cm^3/s
R = column radius, cm

This equation is easily solved for $C(z)$. We obtain

$$C(z) = C_0 \exp(kz) \tag{3}$$

where C_0 = bulk liquid protein concentration at the bottom of the column, mg/cm^3

$k = 3QK/(Dr\pi R^2)$, cm^{-1}

The average bulk protein concentration over the entire column is defined as

$$\bar{C} = \int_0^H C(z)dz / \int_0^H dz \tag{4}$$

This can be integrated to give

$$\bar{C} = C_0 \frac{e^{kH} - 1}{kH} \tag{5}$$

Rearranging gives

$$C_0 = \bar{C}kH/(e^{kH} - 1) \tag{6}$$

which, on substitution into Eq. (3), yields

$$C(z) = \frac{\bar{C}kH \exp(kz)}{\exp(kH) - 1} \tag{7}$$

This can be written as

$$\log_e C(z)/\bar{C} = \log_e \frac{kH}{\exp(kH) - 1} + kz$$

Therefore a plot of log $[C(z)/\bar{C}]$ versus z permits one to determine k from either the slope or the y-intercept. This can therefore be used to check the internal consistency of the data. To make this method of estimating k meaningful, however, would require more data points (i.e., additional sampling ports) than were used in our system. We have one central data point plus the concentrations at the top and bottom of the column to determine the slope and intercept of the linear logarithmic plot; with data

from more sampling locations one could use a linear least squares approach for calculating k.

Alternatively, Eq. (2) can be obtained by performing a shell balance over a slab of thickness δz at steady-state. This approach is more general than that used above, since it can be extended to include unsteady-state conditions and terms representing synthesis or degradation of protein. We obtain

$$\left(\frac{3QK}{r\pi R^2}C - D\frac{dC}{dz}\right)\Bigg|_z - \left(\frac{3QKC}{r\pi R^2} - D\frac{dC}{dz}\right)\Bigg|_{z+\delta z} = 0 \tag{8}$$

Dividing throughout by δz, rearranging terms, and taking the limit as δz approaches 0 then yields

$$\frac{d^2C}{dz^2} - k\frac{dC}{dz} = 0 \tag{9}$$

where, as before,

$$k = 3QK/Dr\pi R^2$$

Equation (9) is readily integrated, with the assumption that k is constant. The boundary conditions are $C(0) = C_b$ at the bottom of the fermentor and $C(H) = C_t$ at the top. The solution can be expressed in dimensionless and normalized form by

$$X(z) = \frac{C(z) - C_b}{C_t - C_b} = \frac{\exp(kz) - 1}{\exp(kH) - 1} \tag{10}$$

where X = a dimensionless, normalized concentration variable.

An alternative but equivalent relationship, involving the separation ratio term which is often used in the bubble fractionation literature, is given by

$$X(z) = \frac{C(z)/C_b - 1}{SR - 1} \tag{11}$$

where SR = separation ratio = C_t/C_b.

Note that from Eq. (3), $SR = \exp(kH)$ and $C - C_b = \exp(kz)$, so Eqs. (10) and (11) match term by term. Equation (10) can also be written in terms of a dimensionless height $Z = z/H$ as follows:

$$X = \frac{\exp(kHZ) - 1}{\exp(kH) - 1} \tag{12}$$

Equation (12) is graphed in Figs. 2-4 for various values of kH (in our examples, $H = 34.5$ cm). The upper diagonal line represents the case where $kH = 0$; L'Hospital's rule yields $X = Z$ from Eq. (12) for this case. Data (*3*) from one enzyme (invertase) bubble fractionation experiment (Experiment 1) and four fermentation-produced protein fractionation experiments (Experiments 2-5) are grouped at the $z/H = 0.5$ positions in the figures. The concentrations at the bottom and top of the column are used to normalize the concentration at the midpoint of the column—that is, to

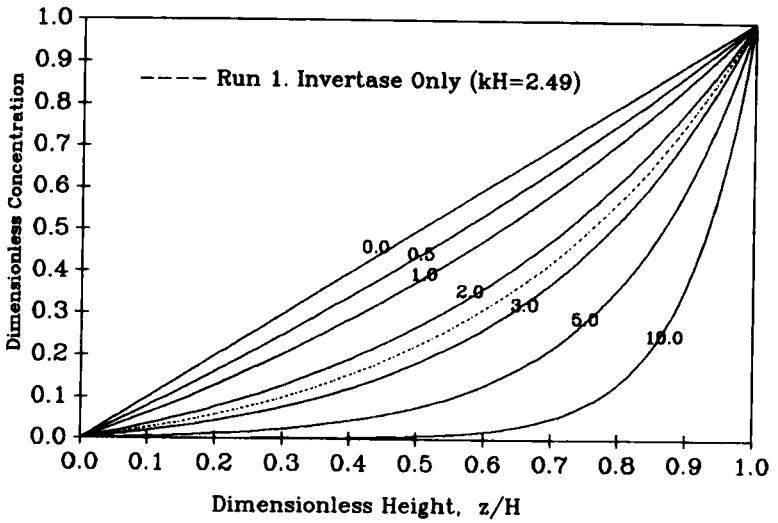

FIG. 2. Bubble fractionation of invertase for a nonfermentation system. Here the sparged CO_2 flow rate was 140 mL/min.

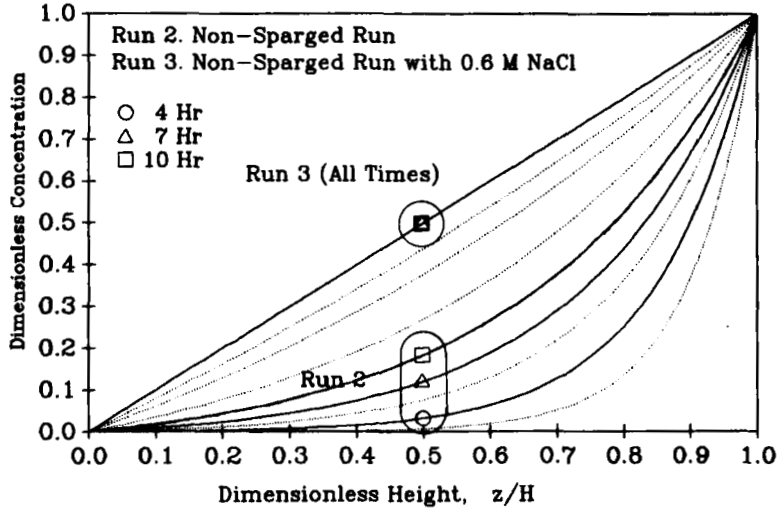

FIG. 3. Total protein concentration profiles in an unsparged system.

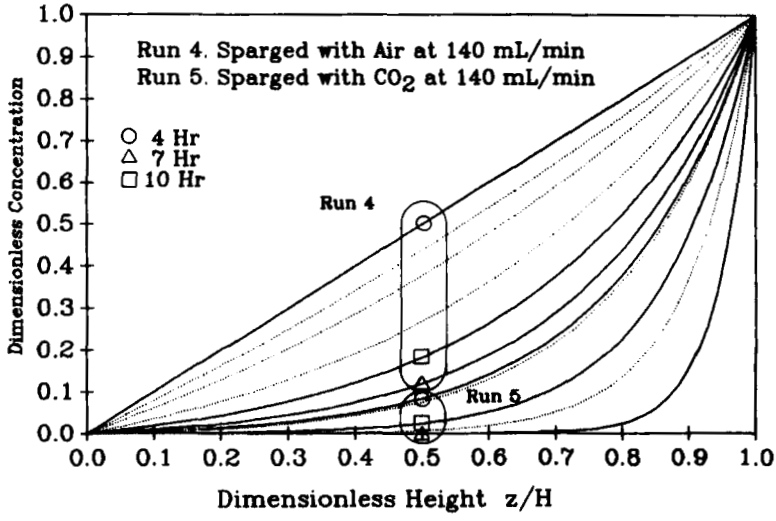

FIG. 4. Total protein concentration profiles in a gas-sparged system.

calculate $X = X(H/2)$. The quantity kH can then be determined from Eq. (12); $kH = 2 \ln (1/X - 1)$.

The constant k in Eqs. (10) and (12) depends on Q, K, D, r, and R. The isotherm constant K is dependent on the types of protein being fractionated; this is affected by the yeast age and the carbon and nitrogen sub-

strates. The dispersion constant D depends upon the column dimensions and alignment, the gas flow rate and gas dispersion head design, and the bubble size.

Since Eq. (12) is a normalized relationship, it, by itself, cannot be used to distinguish between a linear concentration gradient of protein and no concentration gradient at all. This point is illustrated by the data presented. At early stages in the aerated run (Experiment 4, Fig. 4), the protein concentration at the top of the column is 21% greater than that at the bottom. However, the gradient is nearly linear, with a resulting kH value near zero. Experiment 3 (Fig. 3), performed with salt added to the broth, showed no protein concentration gradient within the reactor, so the kH value for this run is also near zero. This observation can be seen directly from the integrated form of Eq. (9) for $k = 0$:

$$C = C_b + \left(\frac{C_+ - C_b}{H}\right) z$$

i.e., $X = Z$.

ALTERNATIVE DERIVATION OF THE MATHEMATICAL MODEL

The following is an alternative derivation of Eq. (9) for the case where the bubble boundary layer thickness is appreciable. It is also more in keeping with contemporary practice in the field of bubble and foam fractionation. It leads to essentially the same result as Eq. (10), but with a somewhat different interpretation for the parameter k. Here, movement of the proteins axially within the column only occurs by bubble transport, so there is no dispersion term *per se.* In this model, proteins are carried upward either by being adsorbed on the surface of a bubble or by entrainment in the boundary layer of liquid surrounding the bubble. Proteins are carried downward in the liquid flow which balances the upward flow of boundary layer liquid.

We partition the column into a set of horizontal slabs of thickness δz, and assume that each slab is perfectly mixed. The gas flow rate is Q mL/s, and the radius of the bubbles is r cm. We assume that each bubble carries with it a boundary layer of liquid of thickness $(b - r)$, where b is the effective outer radius of the spherical boundary layer. Also, N, the number of bubbles transported per second, is given by

$$N = 3Q/4\pi r3$$

We assume local equilibrium within each slab between the surface phase and the bulk solution with respect to protein, and use Eq. (1) to relate surface and bulk protein concentrations.

The mass of protein carried into the ith slab from below [the $(i-1)$ th slab] by a single bubble is given by

$$4\pi r^2\Gamma_{i-1} + \frac{4\pi}{3}(b^3 - r^3)C_{i-1} \tag{13}$$

The mass of protein carried out of the ith slab by the rising bubble and its boundary layer is

$$4\pi r^2\Gamma_i + \frac{4\pi}{3}(b^3 - r^3)C_i \tag{14}$$

The mass of protein carried into the ith slab from above by the flow of liquid counter to the rising bubble boundary layer is

$$\frac{4\pi}{3}(b^3 - r^3)C_{i+1} \tag{15}$$

And the mass of protein carried downward from the ith slab by the flow counter to the rising boundary layer is

$$\frac{4\pi}{3}(b^3 - r^3)C_i \tag{16}$$

On noting that N bubbles pass through the slab boundaries per second, we then obtain for the protein mass balance

$$\frac{dm_i}{dt} = \frac{3Q}{4\pi r^3}\left[4\pi r^2 K(C_{i-1} - C_i) + \frac{4\pi}{3}(b^3 - r^3)(C_{i-1} - 2C_i + C_{i+1})\right] \tag{17}$$

To a very good approximation,

$$m_i = \pi R^2 \delta z C_i = A\delta z C_i \tag{18}$$

So

$$\frac{dC_i}{dt} = -\frac{3QK}{rA}\frac{C_i - C_{i-1}}{\delta z} + \frac{Q\delta z(b^3 - r^3)}{r^3A(\delta z)^2}(C_{i-1} - 2C_i + C_{i+1}) \quad (19)$$

Writing the concentration difference as derivatives then yields

$$\frac{\partial C}{\partial t} = -\frac{3QK}{rA}\frac{\partial C}{\partial z} + \frac{Q\delta z}{A}\frac{b^3 - r^3}{r^3}\frac{\delta^2 C}{\partial z^2} \quad (20)$$

Under quasi-steady-state conditions this becomes

$$-\frac{3QK}{rA}\frac{dC}{dz} + \frac{Q\delta z(b^3 - r^3)}{Ar^3}\frac{d^2C}{dz^2} = 0 \quad (21)$$

or

$$\frac{d^2C}{dz^2} - k'\frac{dC}{dz} = 0 \quad (22)$$

where k' is in units of cm^{-1}:

$$k' = \frac{3Kr^2}{\delta z(b^3 - r^3)}$$

Equation (22) is essentially the same as Eq. (9), so it gives the same concentration profile as described by Eq. (10), but with k' in place of k. Note that the flow rate dependence drops out for the quasi-steady-state case.

In the above expression for k', δz is a dispersion length, and $(b - r)$ describes the thickness of the liquid boundary layer carried along by the bubble. The dispersion coefficient, D, in Eq. (2) is given in the alternate derivation (to equate k to k') by

$$D = \frac{b^3 - r^3}{r^3}\frac{Q}{\pi R^2}\delta z \quad (23)$$

As before, the protein concentration at a height z in the column is given by

$$C(z) = C_0 \exp(k'z) \tag{24}$$

Since

$$\bar{C} = C_0 \frac{[\exp(k'H) - 1]}{k'H} \tag{25}$$

we then have

$$C(z) = \frac{k'H\bar{C} \exp(k'z)}{\exp(k'H) - 1} \tag{26}$$

DISCUSSION

For a system containing microorganisms generating and utilizing extracellular proteins, the ratio of K/D, and k (or k') itself, may change with time. When the protein synthesis and degradation terms are omitted in the model, one may find that k varies to accommodate these changes in protein characteristics. This is seen for the data presented for three out of four of the experiments depicted in Figs. 3 and 4. Only Experiment 3 (with added NaCl) yields values of kH which are constant during the entire course of the fermentation. If one has one or more sampling points at intermediate positions along the column, one can obtain values of k by least squares or graphically. We used Tool Kit Solver Plus for all calculations and generation of all plots.

For the invertase separation (Experiment 1), the data shown in Fig. 2 yield a value of kH of 2.49, so $k = 0.072\ \text{cm}^{-1}$. For the two non-aerated fermentations plotted in Fig. 3, poorer separation resulted for the run in which NaCl was present, (Experiment 3, for which $kH = 0.034$, essentially zero.) Substantially better separation occurred when no added salt was present, (Experiment 2, for which $3 < kH < 7$ during the course of the run). Figure 4 presents the data for two sparged runs; gassing with CO_2 greatly enhances the separation (Experiment 5, $5 < kH < 17$), and separation is enhanced somewhat for aerated systems for times between 7 and 10 h only (Experiment 4, $2.5 < kH < 3.5$). On examining the expression for k ($k = 3QK/Dr\pi R^2$), one concludes that the effect of salt is probably due to its reducing K, since D probably is virtually unaffected and the bubble radius is likely to be changed only slightly.

Yeast fermentation generates constitutive and induced proteins as well as other compounds, such as ethanol. The rate of extracellular protein

production is important, especially in genetic engineering applications where products such as insulin or interferon may be synthesized, but the extracellular production rate may be difficult to determine if the average bulk concentration of the product as a function of time is not known. A single sampling point does not provide an accurate measure of the average protein concentration if bubble fractionation is occurring. By using Eqs. (24) and (25), one can estimate the average protein concentration from a minimum of two sample points without mixing the liquid broth and thereby disturbing the concentration gradient.

One can also use the reduced variable X defined in Eq. (10) for the calculation. We illustrate this with the invertase separation plotted in Fig. 2. Here the invertase concentrations after 20 min of aeration are 0.041, 0.075, and 0.193 g/L at z/H: 0, 0.5, and 1, respectively. The average value of X is given by

$$\bar{X} = \frac{1}{kH} - \frac{1}{\exp(kH) - 1} \tag{27}$$

and $kH = 2.49$ for this run. This yields $\bar{X} = 0.311$ from Eq. (27), and $\bar{C} = 0.0883$ g/L. The experimentally measured concentration at the middle of the column was 0.075 g/L, and the column was charged with a solution containing 0.095 g/L. The average value obtained from the model is substantially closer to the true average concentration than is the midpoint concentration, which is off by 21% from the correct value. Additional sampling points along the length of the reactor should result in further improvement in the calculated average concentration, since the value of k would be known with greater accuracy.

For this type of process it is desirable to monitor the generation rate of the protein of interest. This requires an accurate value of the average concentration within the bioreactor. The model described here, together with a quite limited number of protein concentration measurements, provides such values. By sampling the column at various times, the protein concentrations can be monitored to determine the optimal reactor operating time for either maximum total product concentration or for maximum product concentration gradient.

The observed protein concentration gradients suggest that there may be an optimum volume of supernatant to remove for further processing or purification. This top volume aliquot could represent a given percentage of the total protein in the reactor, or it might be chosen to be enriched to a certain concentration in a particular protein. In our invertase separation,

if we wish to remove a top aliquot which contains a concentration of C_u g/L, this should be taken at a height L, where L is calculated numerically from

$$C_u = \frac{H\bar{C}}{[\exp(kH) - 1]} \frac{\exp(kH) - \exp(kL)}{H - L} \tag{28}$$

For the invertase separation, if we choose $C_u = 0.16$ g/L, then solution of Eq. (28) yields $L = 19.8$ cm.

Specific proteins may exhibit much larger concentration gradients than the bulk protein at any given time. The data suggest that there is often an optimum time to harvest the upper layer for a desired protein. In this connection one might be able to maximize K by adjustment of the pH to the isoelectric point of the desired protein, thereby increasing its surface activity.

We note that the model is an approximation to which one should append protein synthesis and degradation terms. This should result in a decrease in the variation of k with time in the fermentation experiment simulations (Experiments 2, 4, and 5).

Carbon dioxide seems to enhance the protein separation as evidenced by the high kH values in both Experiment 2 (natural CO_2 evolution; see Fig. 3) and Experiment 5 (CO_2 sparging; see Fig. 4).

CONCLUSIONS

High axial protein concentration gradients can be achieved by means of bubble fractionation with carbon dioxide, either generated by fermentation or supplied externally. The presence of salt, on the other hand, reduces the efficiency of bubble fractionation. Protein bubble fractionation can be described by means of a steady-state model for which parameters can readily be estimated from experimental data and which can be used to optimize separations.

Acknowledgment

The authors are grateful to Dr. Robert J. Roselli for his guidance in the development of the model. Thanks are also due to Adosh Mehta and S. R. Chakravarthy for their assistance in the preparation of this manuscript.

REFERENCES

1. D. H. Park, D. S. Baker, K. G. Brown, R. D. Tanner, and G. W. Malaney, *J. Biotechnol., 2,* 337–346 (1985).
2. W. T. Effler Jr., N. K. Pandey, R. D., Tanner, and G. W. Malaney, *Biotechnol. Bioeng. Symp., 17,* 633–643 (1986).
3. W. T. Effler, R. D. Tanner, and G. W. Malaney, "Dynamic *in-situ* Fractionation of Extracellular Proteins Produced in a Baker's Yeast Cultivation Process," in *Bioproducts and Bioprocesses* (A. Fiechter, H. Okada, and R. D. Tanner, eds.), Springer Verlag, 1989, pp. 235–256.

Received by editor September 13, 1989